Chen-Hu, K. & Garcia Armada, A. (2019). *Non-Coherent Multiuser Massive MIMO-OFDM with Differential Modulation*. In: ICC 2019 - 2019 IEEE International Conference on Communications (ICC), 20-24 may, 2019, Shanghai.

DOI: 10.1109/icc.2019.8761447

Non-Coherent Multiuser Massive MIMO-OFDM with Differential Modulation

Kun Chen-Hu and Ana Garcia Armada
Department of Signal Theory and Communications, Universidad Carlos III de Madrid (Spain)
E-mail: {kchen, agarcia}@tsc.uc3m.es

***Abstract*—Massive multiple-input multiple-output (MIMO) and orthogonal frequency division multiplexing (OFDM) are wireless technologies adopted by the Fifth Generation (5G) of mobile communications. The channel estimation and pre/post-equalization processes in coherent detection schemes for massive MIMO-OFDM are a challenging task, where several issues are faced, such as pilot contamination, channel calibration, matrix inversions, among others. Moreover, they increase the energy consumption and latency of the system. A non-coherent technique relying on DPSK constellation has been proposed for a single-carrier scheme, assuming flat-fading. In our paper, we extend this technique to be combined with OFDM, where the channel is doubly dispersive (time and frequency). We will show that the differential modulation can be performed either in the time or frequency domain, where the latter suffers from an additional phase rotation, which should be estimated and compensated. We provide the analytical expression of the signal-to-interference-and-noise ratio (SINR) for both cases, and we show numerical results in order to verify our analysis.**

I. Introduction

The Fifth Generation (5G) of mobile communications [1] has just standardized a New Radio (NR), where massive multiple-input multiple-output (MIMO) [2] and orthogonal frequency division multiplexing (OFDM) [3] are the chosen techniques to deploy new services, such as enhanced mobile broadband (eMBB), massive machine type communications (mMTC) and ultra-reliable and low latency communications (URLLC).

When a coherent demodulation scheme is adopted, a significant amount of orthogonal pilot sequences need to be transmitted allowing the estimation of the channel between each user equipment (UE) and each antenna of the base station (BS), in every time-frequency resource, reducing the overall capacity. Moreover, the number of available orthogonal sequences is limited, forcing us to reuse them [4], and creating the well-known pilot contamination issue [5]. Once the pilot sequences are received, the receiver must estimate the channel avoiding, as far as possible, any source of interference, and compute the pre/post-equalizers. Either of the processes requires several prohibitive matrix inversions when the number of antennas is high [6], increasing the power consumption and latency. According to the literature, when massive MIMO is adopted, time division duplex (TDD) is preferred rather than frequency division duplex (FDD) [7], due to the fact that the former can take advantage of the channel reciprocity, where the channel estimation is done in the uplink (UL), and it is reused in the downlink (DL). Therefore, the pilot overhead is reduced. However, there is plenty of FDD spectrum for wireless communications today.

Given the mentioned issues, an alternative way is the use of non-coherent schemes. [8] has proposed this idea with the use of amplitude shift keying (ASK). However, the number of required antennas is excessively large for a reasonable performance. Later, [9] proposed the use of differential phase shift keying (DPSK), where two received contiguous symbols are properly combined in order to produce a joint-symbol. The final decision is done on this joint-symbol, which is a superposition of the transmitted symbol of each UE. This proposal significantly outperforms [8], showing that it does not require a huge number of antennas in order to achieve an acceptable performance. However, this scheme is implemented with single-carrier modulation (SCM), assuming that the channel is flat-fading and remains invariant over a long-enough coherence time. The effect of time-varying channels is also analyzed in [10] for the case of SCM systems, where it is concluded that the non-coherent scheme is robust to fast time variability of the channel.

For more realistic cases where the propagation channel is doubly dispersive, in this paper we propose the extension of the scheme [9] to the use of OFDM. Additionally, due to the fact that OFDM implements a two dimensional resource grid, the differential encoding can be performed in either time or frequency domain, where we define them as time domain scheme (TDS) and frequency domain scheme (FDS), respectively. Comparing both schemes, TDS requires two OFDM symbols in order to perform the differential decoding, increasing the memory consumption and latency of the system. Hence, TDS has some shortcomings for either mMTC or URLLC. In FDS, the differential encoding can be performed for each pair of contiguous subcarriers, overcoming the mentioned disadvantages of TDS. However, the difference of the phase between the two contiguous subcarriers is not averaged out by the large number of antennas at the BS, causing an additional rotation in the received joint-symbol. Therefore, FDS needs a phase estimation method to compensate it. We develop such a scheme and we provide the expression of the signal-to-interference-and-noise ratio (SINR) for both cases. We also show some numerical results of the symbol error rate (SER) of different schemes, using the channel models provided by [1].

The remainder of the paper is organized as follows. Section II provides the system model of MIMO-OFDM with the use of

DPSK. Section III describes the receiver of TDS and provides the analytical expression of the SINR under a time-varying channel response. Section IV shows the receiver of FDS, the analytical expression of the SINR under the presence of multipath is also given, and a phase estimation method is presented. Section V presents some numerical results to verify our theoretical analysis and provides a better understanding of the system performance. Finally, in section VI, some conclusions are pointed out.

Notation: matrices, vectors and scalar quantities are denoted by boldface uppercase, boldface lowercase, and normal letters, respectively. $[\mathbf{A}]_{m,n}$ denotes the element in the m-th row and n-th column of $\mathbf{A}$. $[\mathbf{a}]_n$ represents the n-th element of vector $\mathbf{a}$. The superscripts $(\cdot)^H$, $(\cdot)^*$ denote Hermitian and complex conjugate, respectively. $*$ denotes the convolution operation. $\mathbb{E}\{\cdot\}$ represents the expected value. $\mathcal{CN}(0,\sigma^2)$ represents the circularly-symmetric and zero-mean complex normal distribution with variance σ^2.

II. System Model

A. MIMO-OFDM

We consider a multiuser MIMO-OFDM system, which is made up of one BS equipped with an array of V antennas and U UE equipped with one single antenna each (see Fig. 1). The OFDM signal has K subcarriers and the length of the cyclic prefix (CP) is long enough to absorb the effects of the multi-path channel. We focus on the UL. At the receiver side, after removing the CP and performing a fast-Fourier transform (FFT) to each block at each antenna of the BS, we can process each subcarrier as one of a set of K independent sub-channels.

We assume that the U UEs transmit M consecutive OFDM symbols to the BS. The received signal at the BS in the k-th subcarrier and m-th time instant $\mathbf{y}_k^m\,(V\times 1)$ can be modeled as

$$\mathbf{y}_k^m = \mathbf{H}_k^m\mathbf{D}\mathbf{x}_k^m + \mathbf{w}_k^m \quad 1\le k\le K, \quad 1\le m\le M, \quad (1)$$

where

$$[\mathbf{D}]_{u,u'} = \begin{cases} \sqrt{d_u} & u=u' \\ 0 & u\neq u' \end{cases}, \quad 1\le u,u'\le U, \quad (2)$$

$$\mathbf{x}_k^m = \left[[\breve{\mathbf{x}}_1^m]_k \quad \cdots \quad [\breve{\mathbf{x}}_U^m]_k\right]^T, \quad (3)$$

$$\mathbf{w}_k^m = \left[[\breve{\mathbf{w}}_1^m]_k \quad \cdots \quad [\breve{\mathbf{w}}_V^m]_k\right]^T, \quad (4)$$

$$\mathbf{H}_k^m = \begin{bmatrix} \left[\tilde{\mathbf{h}}_{11}^m\right]_k & \cdots & \left[\tilde{\mathbf{h}}_{1U}^m\right]_k \\ \vdots & \ddots & \vdots \\ \left[\tilde{\mathbf{h}}_{V1}^m\right]_k & \cdots & \left[\tilde{\mathbf{h}}_{VU}^m\right]_k \end{bmatrix}, \quad \tilde{\mathbf{h}}_{vu}^m = \mathbf{F}_K\mathbf{h}_{vu}^m, \quad (5)$$

$$[\mathbf{F}_K]_{a,b} = \frac{1}{\sqrt{K}}\exp\left(-j\frac{2\pi}{K}(a-1)(b-1)\right), \quad (6)$$

d_u is the average power of the signal of u-th UE, $\breve{\mathbf{x}}_u^m\,(K\times 1)$ represents the transmitted symbol vector from the single antenna of the u-th UE in the m-th OFDM symbol, with unit average power; $\breve{\mathbf{w}}_v^m\,(V\times 1)$ denotes the additive white Gaussian noise (AWGN) vector in the frequency domain with each element distributed according to $[\breve{\mathbf{w}}_v^m]_k \sim \mathcal{CN}(0,\sigma_w^2)$; $\tilde{\mathbf{h}}_{vu}^m\,(K\times 1)$ and $\mathbf{h}_{vu}^m\,(L_{CH}\times 1)$ are the channel response in the frequency and time domain, respectively. The distribution of the channel frequency response at each subcarrier follows $\left[\tilde{\mathbf{h}}_{vu}^m\right]_k \sim \mathcal{CN}(0,1)$ due to the fact that the power delay profile (PDP) of $\mathbf{h}_{vu}^m$ is normalized.

Additionally, we assume that the channel suffers from time variability, where

$$\mathbb{E}\left\{\left|([\mathbf{h}_{vu}^m]_l)^*\left[\mathbf{h}_{vu}^{m'}\right]_l\right|\right\} = \left|J_0\left(2\pi f_{d,u}\frac{\Delta m}{\Delta f}\left(1+\frac{L_{CP}}{K}\right)\right)\right|, \quad \Delta m = m'-m\in\mathbb{N}, \quad 1\le l\le L_{CH}, \quad (7)$$

where $J_0(\cdot)$ denotes the zero-th order Bessel function of the first kind, $f_{d,u}$ and Δf represent the Doppler frequency experienced by the signal transmitted from the u-th and the distance between two contiguous subcarriers, respectively, measured in Hz.

B. Differential Modulation

According to [9], in order to implement the non-coherent MIMO system, a differential modulation scheme is needed. Given an OFDM system, the differential encoding can be performed either in time or frequency domain (TDS or FDS).

In TDS, each symbol $[\breve{\mathbf{x}}_u^m]_k$ can be obtained as

$$[\breve{\mathbf{x}}_u^m]_k = \left[\breve{\mathbf{x}}_u^{m-1}\right]_k[\mathbf{s}_u^m]_k, \quad 2\le m\le M, \quad 1\le k\le K, \quad 1\le u\le U, \quad (8)$$

where $[\mathbf{s}_u^m]_k$ belongs to a DPSK constellation as we see in the next subsection, and $\left[\breve{\mathbf{x}}_u^{m=1}\right]_k$ is a reference symbol. However, at the receiver side, TDS requires waiting for the reception of two complete OFDM symbols in order to obtain $\mathbf{s}_u^m$, due to the fact that it performs a differential decoding of two contiguous symbols in the time domain, as we see in the following subsection. Hence, it increases both the memory consumption and the latency of the system. When K is high this scheme is not recommendable for either mMTC or URLLC.

In FDS, applying the same philosophy, each symbol $[\breve{\mathbf{x}}_u^m]_k$ can be obtained as

$$[\breve{\mathbf{x}}_u^m]_k = [\breve{\mathbf{x}}_u^m]_{k-1}[\mathbf{s}_u^m]_k, \quad 2\le k\le K, \quad 1\le m\le M, \quad 1\le u\le U, \quad (9)$$

where $[\breve{\mathbf{x}}_u^m]_{k=1}$ is a reference symbol. With this scheme, the disadvantages related to the memory consumption and the latency are mitigated.

At the receiver, the phase difference of two consecutive symbols received (either time or frequency) at each antenna of the BS is non-coherently detected. Then, they are all added in order to provide the joint-decision variable (joint-symbol), which is obtained from the superimposed combinations of the individual symbol of each UE (see Fig. 1).

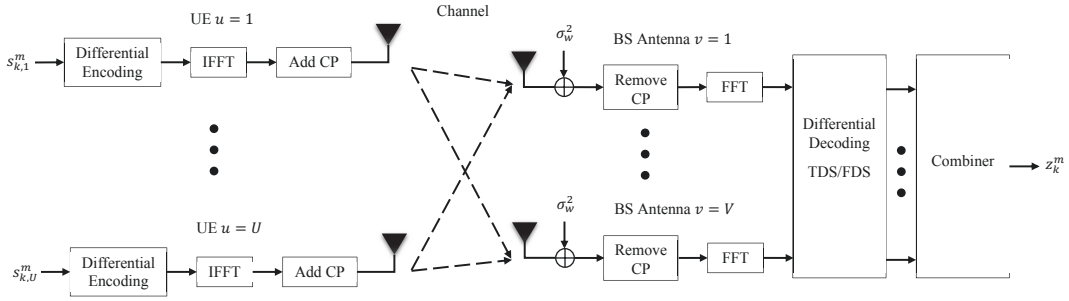

Fig. 1. Block diagram of the non-coherent multiuser massive MIMO-OFDM.

C. Constellation

The symbols transmitted by each UE $[\mathbf{s}_u^m]_k$ belong to a G-ary DPSK constellation that has to be designed to guarantee that the joint symbol allows a unique demodulation of them. For illustration purposes, we select the constellation type B given in [9] (see Fig. 2), due to the fact that it outperforms the type A. Then, the UEs transmit symbols from a standard constellation, defined as

$$[\mathbf{s}_u^m]_k \in \mathcal{G}_u = \left\{ \frac{2\pi g}{G}, \quad g = 0, 1, \ldots, G-1 \right\}. \tag{10}$$

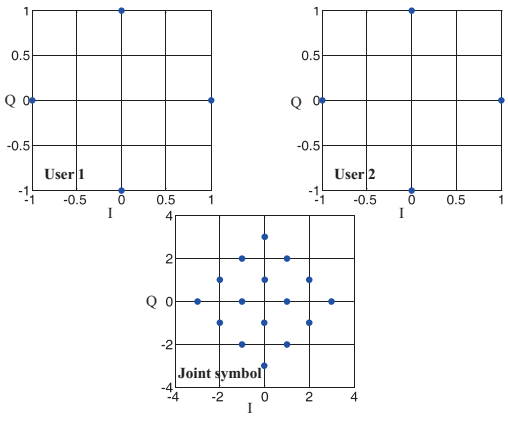

Fig. 2. Constellation type B of [9], where $U = 2$, $d_1 = 1$ and $d_2 = 2$.

III. Time Domain Scheme

At the receiver, we combine two contiguous symbols in the time domain for a given k-th subcarrier and each antenna, then we sum all of them as

$$\begin{aligned} z_{t,k}^m &= \frac{1}{V} \left(\mathbf{y}_k^{m-1}\right)^H \mathbf{y}_k^m = \\ &= \frac{1}{V} \Big(\left(\mathbf{x}_k^{m-1}\right)^H \mathbf{D} \left(\mathbf{H}_k^{m-1}\right)^H \mathbf{H}_k^m \mathbf{D} \mathbf{x}_k^m + \left(\mathbf{w}_k^{m-1}\right)^H \mathbf{w}_k^m + \\ &+ \left(\mathbf{x}_k^{m-1}\right)^H \mathbf{D} \left(\mathbf{H}_k^{m-1}\right)^H \mathbf{w}_k^m + \left(\mathbf{w}_k^{m-1}\right)^H \mathbf{H}_k^m \mathbf{D} \mathbf{x}_k^m \Big). \end{aligned} \tag{11}$$

and from this decision variable $z_{t,k}^m$, we will detect the symbol transmitted by each UE.

We define $\rho_{t,u}$ as

$$\rho_{t,u} = \frac{1}{V} \mathbb{E} \left\{ \sum_{v=1}^{V} \left(\left[\tilde{\mathbf{h}}_{vu}^{m-1} \right]_k \right)^* \left[\tilde{\mathbf{h}}_{vu}^m \right]_k \right\}, \tag{12}$$
$$1 \le k \le K, \quad 1 \le m \le M, \quad 1 \le u \le U.$$

Substituting (7) in (12), we can easily obtain

$$\rho_{t,u} = \left| J_0 \left(\frac{2\pi f_{d,u}}{\Delta f} \left(1 + \frac{L_{CP}}{K} \right) \right) \right|. \tag{13}$$

Moreover, by exploiting the properties of Wishart matrices [11], we can see that

$$\mathbb{E} \left\{ \left| \sum_{v=1}^{V} \left(\left[\tilde{\mathbf{h}}_{vu}^{m-1} \right]_k \right)^* \left[\tilde{\mathbf{h}}_{vu}^m \right]_k \right|^2 \right\} = \rho_{t,u}^2 V (V+1). \tag{14}$$

Making use the Law of Large Numbers, we have that

$$\frac{1}{V} \left(\mathbf{H}_k^{m-1}\right)^H \mathbf{H}_k^m \in \mathbb{C}^{U \times U} \xrightarrow{V \to \infty} \mathbf{P}_t, \tag{15}$$

$$[\mathbf{P}_t]_{u,u'} = \begin{cases} \rho_{t,u} & u = u' \\ 0 & u \neq u' \end{cases}, \quad 1 \le u, u' \le U. \tag{16}$$

This means that

$$z_{t,k}^m \xrightarrow{V \to \infty} r_{t,k}^m = \sum_{u=1}^{U} \rho_{t,u} d_u \left[\mathbf{s}_u^m\right]_k, \tag{17}$$

where $r_{t,k}^m$ denotes the joint-symbol, which is obtained as a weighted sum of the transmitted symbol of each UE, where the weight coefficients are their average power and channel correlation between two consecutive time instants. For the particular case of $\rho_{t,u} = 1, \ \forall u \in \{1, 2, \ldots U\}$, $r_{t,k}^m$ corresponds with the definition of the joint-symbol of [9].

A. Analysis of the SINR

When V is not large enough for (15) and (16) to hold, we have some interference and noise terms i_k^m that can be characterized as

$$i_k^m = \sum_{u=1}^{U} d_u \left[\mathbf{s}_u^m\right]_k - z_{t,k}^m, \tag{18}$$

The full expression of i_k^m (19) is given in the next page.

By applying (12) and (14), the expression of the SINR is given by (20). When the channel is quasi-stationary in any

$$
\begin{aligned}
i_k^m = & \sum_{u=1}^{U} d_u \left[\mathbf{s}_u^m\right]_k \left(1 - \frac{1}{V}\sum_{v=1}^{V}\left(\left[\tilde{\mathbf{h}}_{vu}^{m-1}\right]_k\right)^* \left[\tilde{\mathbf{h}}_{vu}^{m}\right]_k\right) - \\
& - \frac{1}{V}\sum_{u=1}^{U}\sum_{\substack{u'=1\\u'\neq u}}^{U}\sum_{v=1}^{V}\left(\left[\tilde{\mathbf{h}}_{vu}^{m-1}\right]_k\right)^* \left[\tilde{\mathbf{h}}_{vu'}^{m}\right]_k \sqrt{d_u d_{u'}}\left(\left[\breve{\mathbf{x}}_u^{m-1}\right]_k\right)^* \left[\breve{\mathbf{x}}_{u'}^{m}\right]_k - \frac{1}{V}\sum_{v=1}^{V}\left(\left[\breve{\mathbf{w}}_v^{m-1}\right]_k\right)^* \sum_{u=1}^{U}\left[\tilde{\mathbf{h}}_{vu}^{m}\right]_k \sqrt{d_u}\left[\breve{\mathbf{x}}_u^{m}\right]_k - \\
& - \frac{1}{V}\sum_{v=1}^{V}\left[\breve{\mathbf{w}}_v^{m}\right]_k \sum_{u=1}^{U}\left(\left[\tilde{\mathbf{h}}_{vu}^{m-1}\right]_k\right)^* \sqrt{d_u}\left(\left[\breve{\mathbf{x}}_u^{m-1}\right]_k\right)^* - \frac{1}{V}\sum_{v=1}^{V}\left(\left[\breve{\mathbf{w}}_v^{m-1}\right]_k\right)^* \left[\breve{\mathbf{w}}_v^{m}\right]_k .
\end{aligned}
\tag{19}
$$

$$
\mathrm{SINR}_{TDS} = \frac{\sum_{u=1}^{U} d_u^2}{\sum_{u=1}^{U} d_u^2\left(1 - 2\rho_{t,u} + \left(1+\frac{1}{V}\right)\rho_{t,u}^2\right) + \frac{1}{V}\left(2\sum_{u=1}^{U}\sum_{u'=u+1}^{U} d_u d_{u'} + 2\sigma_w^2\sum_{u=1}^{U} d_u + \sigma_w^4\right)}
\tag{20}
$$

of the V links between the u-th UE and BS ($\rho_{t,u} = 1\ \forall u \in \{1, 2, \dots U\}$), (20) has the same expression as the SINR given in [9], where the large number of antennas at the BS will reduce the interference and noise terms. On the other hand, when the channel response of all links suffers from a very high time variability ($\rho_{t,u} = 0\ \forall u \in \{1, 2, \dots U\}$), the first term of the denominator of (20) is no longer attenuated by the factor V, making the interference and noise even be higher than the signal term. These are of course two extreme cases. In general $0 \leq \rho_{t,u} \leq 1$ and the performance will worsen as $\rho_{t,u} \to 0$.

IV. Frequency Domain Scheme

Analogously to TDS, but using contiguous subcarriers, the received symbol in the FDS is given by

$$
\begin{aligned}
z_{f,k}^m &= \frac{1}{V}\left(\mathbf{y}_{k-1}^m\right)^H \mathbf{y}_k^m = \\
&= \frac{1}{V}\left(\left(\mathbf{x}_{k-1}^m\right)^H \mathbf{D}\left(\mathbf{H}_{k-1}^m\right)^H \mathbf{H}_k^m \mathbf{D}\mathbf{x}_k^m + \left(\mathbf{w}_{k-1}^m\right)^H \mathbf{w}_k^m + \right. \\
&\left. + \left(\mathbf{x}_{k-1}^m\right)^H \mathbf{D}\left(\mathbf{H}_{k-1}^m\right)^H \mathbf{w}_k^m + \left(\mathbf{w}_{k-1}^m\right)^H \mathbf{H}_k^m \mathbf{D}\mathbf{x}_k^m\right).
\end{aligned}
\tag{21}
$$

where again $z_{f,k}^m$ is the decision variable.

We define the matrix $\mathbf{R}_{f,k}^m$ as

$$
\mathbf{R}_{f,k}^m = \frac{1}{V}\left(\mathbf{H}_{k-1}^m\right)^H \mathbf{H}_k^m \in \mathbb{C}^{U\times U},
\tag{22}
$$

$$
\begin{aligned}
\left[\mathbf{R}_{f,k}^m\right]_{u',u} &= \frac{1}{V}\sum_{v=1}^{V}\left(\left[\tilde{\mathbf{h}}_{vu'}^m\right]_{k-1}\right)^* \left[\tilde{\mathbf{h}}_{vu}^m\right]_k = \\
&= \frac{1}{V}\sum_{v=1}^{V} a_{vu',k-1}^m a_{vu,k}^m \exp\left(j\left(\varphi_{vu,k}^m - \varphi_{vu',k-1}^m\right)\right),
\end{aligned}
\tag{23}
$$

where $\left[\tilde{\mathbf{h}}_{vu}^m\right]_k = a_{vu,k}^m \exp\left(j\varphi_{vu,k}^m\right)$.

Making use the Law of Large Numbers similarly, we have that

$$
\mathbf{R}_{f,k}^m \xrightarrow{V\to\infty} \mathbf{P}_f,
\tag{24}
$$

$$
\left[\mathbf{P}_f\right]_{u,u'} = \begin{cases} \rho_{f,u}\exp\left(j\theta_{f,u}\right) & u = u' \\ 0 & u \neq u' \end{cases},
\tag{25}
$$

$$
\rho_{f,u} = \left|\lim_{V\to\infty}\left[\mathbf{R}_{f,k}^m\right]_{u,u}\right|, \quad \theta_{f,u} = \measuredangle\left(\lim_{V\to\infty}\left[\mathbf{R}_{f,k}^m\right]_{u,u}\right),
\tag{26}
$$

where $\rho_{f,u}$ and $\theta_{f,u}$ are the amplitude and phase of the correlation between the frequency-domain channel responses of two consecutive subcarriers of u-th UE averaged over the V antennas of the BS, respectively. In contrast to TDS, $\theta_{f,u} \neq 0$ even for $V \to \infty$. The reason is as follows.

The coefficients $\mathbf{h}_{uv}^m$ and their inverse are modeled as finite impulse response (FIR) filters, which are stable and causal. According to [12], all the zeros and poles of them are placed inside of the unit circle, making what is commonly known as minimum-phase system. This system is characterized by the fact that the slope of the phase of the frequency-domain response is only positive in the presence of deeply faded subcarriers ($\varphi_{vu,k}^m - \varphi_{vu',k-1}^m > 0$); otherwise it is negative ($\varphi_{vu,k}^m - \varphi_{vu',k-1}^m < 0$).

Taking into account the properties of minimum-phase systems, the deeply faded subcarriers (positive phase) do not make a significant contribution in the sum (23). Hence, if there was only one non-deeply faded link between u-th UE and the V antennas of the BS, it is a sufficient condition to have a negative phase ($\theta_{f,u} < 0$). Hence,

$$
z_{f,k}^m \xrightarrow{V\to\infty} r_{f,k}^m = \sum_{u=1}^{U} \rho_{f,u}\exp\left(j\theta_{f,u}\right) d_u \left[\mathbf{s}_u^m\right]_k ,
\tag{27}
$$

where we can see that FDS requires a mandatory phase estimation and correction.

Assuming that the phase of $z_{f,k}^m$ is properly estimated and corrected at the receiver, the expression of SINR_{FDS} is the same as SINR_{TDS} , substituting $\rho_{t,u}$ by $\rho_{f,u}$.

A. Phase estimation

Here, we undertake the estimation of the phase of $z_{f,k}^m$ by transmitting some pilot-symbols, instead of the unknown

$[\mathbf{s}_u^m]_k$. Given (27), where we have assumed that $V \to \infty$, all the UEs must transmit only one pilot-symbol using the differential modulation at m-th time instant and k-th subcarrier, defined as

$$[\breve{\mathbf{x}}_u^m]_k = [\breve{\mathbf{x}}_u^m]_{k-1}\, p, \quad 1 \le u \le U. \tag{28}$$

where p denotes the pilot-symbol, and the only condition we impose is that the pilot-symbols transmitted by all UEs be the same. Therefore, given our condition in (28), from (27) we obtain

$$r_f^p = p \sum_{u=1}^{U} \rho_{f,u} \exp\left(j\theta_{f,u}\right) d_u \implies \measuredangle r_f^p = \measuredangle p + \measuredangle \psi_f, \tag{29}$$

where r_f^p is the received joint-pilot-symbol, and ψ_f is the phase caused by the selective-fading channel response, that should be corrected from the received data symbols $r_{f,k}^m$.

However, when V is not large enough, (24) - (27) do not hold. Hence, not only the received signal $z_{f,k}^m$ is polluted by the noise and interference terms, but also ψ_f has a different value for each time-frequency resource ($\psi_{f,k}^m$) due to the fact that we are assuming a doubly dispersive channel model. Given these facts, we should estimate $\psi_{f,k}^m$ for each subcarrier (separately) and every time period where the channel remains invariant, so the $\widehat{\psi}_{f,k}^m$ is given by

$$\widehat{\psi}_{f,k'}^m = \frac{1}{K_g} \sum_{\substack{k=1-K_g \\ +K_g k'}}^{K_g k'} \left(\measuredangle\left(z_{f,k}^m\right) - \measuredangle p\right), \quad 1 \le k' \le \left\lceil \frac{K}{K_g} \right\rceil, \tag{30}$$

where averaging K_g neighbor subcarriers helps to reduce the mentioned noise and interference terms provided that they are within the coherence bandwidth of the channel.

V. Numerical Results

In this section, we provide some numerical results for both TDS and FDS. Additionally, we also show the performance of FDS combined our proposed phase estimation technique.

In Table I, we can see the default numerical values for the parameters that we defined in the previous sections. We choose the well-known LTE Extended Vehicular A (EVA) and Extended Typical Urban (ETU) channel models [1] for the PDP, we consider spatially uncorrelated channels and we assume that all UEs are experiencing the same PDP and Doppler frequency f_d. In order to better illustrate the effect of the time variability in the channel response, we additionally set an extreme case of $f_d = 1600$Hz which can be obtained assuming carrier frequency of $f_c = 3.5$GHz and a speed of approximately $v = 500$km/h.

Given that the channel response is doubly dispersive, $\widehat{\psi}_{f,k}^m$ is updated for each frame using (30) for FDS, denoted as realistic case (RC). Moreover, in order to show the accuracy of our proposed RC phase estimation method, we compare it with a benchmark ideal case (IC), where $\widehat{\psi}_{f,k}^m$ is computed directly from the diagonal elements of $\mathbf{R}_{f,k}^m$ without the effects of noise and interference.

TABLE I
Simulation Parameters

K	128	**Constellation**	Type B [10]
Δf	15 KHz	$\mathbf{f_d}$	70, 300 & 1600 Hz
Chan. Model	EVA & ETU	$\mathbf{K_g}$	1 & 2
V	100 & 1000	$\mathbf{L_{CH}}$	5 & 9
U	2	$\mathbf{L_{CP}}$	9
1 Frame = 140 OFDM symbols			

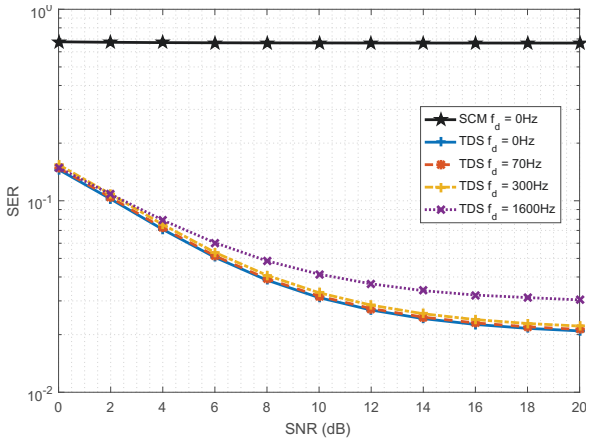

Fig. 3. SER of SCM and TDS for different values of f_d and $V = 100$.

The signal-to-noise ratio (SNR) at any receive antenna of the BS is defined as

$$\text{SNR} = \frac{1}{\sigma_w^2} \sum_{u=1}^{U} d_u. \tag{31}$$

Fig. 3 provides the SER of SCM and TDS for different Doppler frequencies and $V = 100$. In the particular case of SCM [9], the performance is not acceptable when a multi-tap channel response is used; as we expected the single-carrier differential modulation is only effective in flat-fading channels. For the case of OFDM, when the channel remains constant (same assumption as in [9]), the performance is the best. However, the quality of the system is degraded as the Doppler frequency is increased, where the worst performance corresponds to $f_d = 1600$Hz. In any case, for reasonably moderate values of f_d, the performance degradation is negligible as anticipated in [10].

Fig. 4 shows the SER of FDS for different values of PDP and f_d, and $V = 100$. Fig. 4a provides the performance for ETU with $f_d = 1600$Hz, and Fig. 4b illustrates the results for EVA with $f_d = 70$Hz. Comparing them, the additional phase rotation effect in the joint-symbol is greater in those channels with a stronger frequency selectivity, making the processes of phase estimation and correction crucial to obtain a reasonable performance. Additionally, we can see that in both cases, when the phase is estimated and mitigated, the SER is reduced. When $K_g = 2$, that is, averaging only two subcarriers, the RC has almost the same performance as IC, showing that our proposed method is accurate enough to estimate the phase.

Fig. 5 shows the SER comparison for FDS between using only 1 and K pilot-symbols to obtain $\widehat{\psi}_{f,k}^m$ for $V = 100$

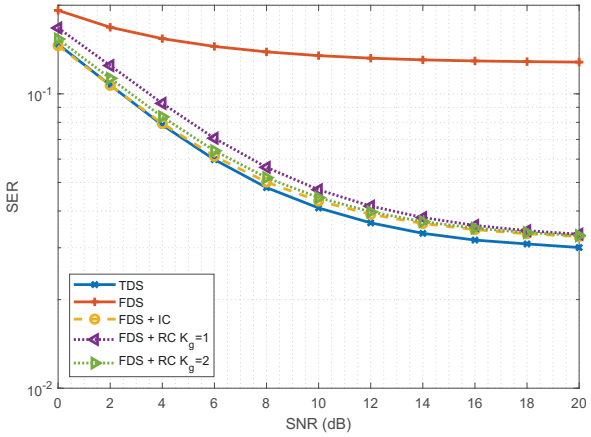

(a) ETU with $f_d = 1600$KHz.

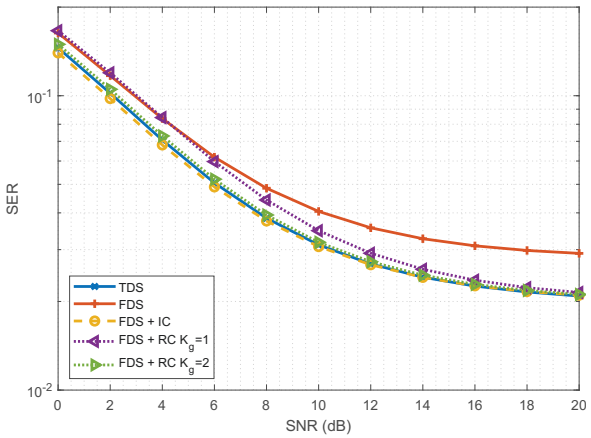

(b) EVA with $f_d = 70$.

Fig. 4. SER of FDS for $V = 100$.

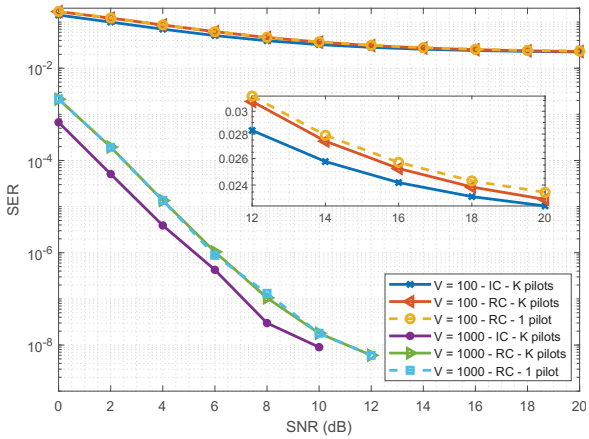

Fig. 5. SER of FDS for ETU with $f_d = 70$Hz and $K_g = 1$.

and 1000. When $V = 100$, using K pilot-symbols provides a slightly better performance as compared to using only 1 pilot-symbol. However, when $V = 1000$, both schemes have the same performance verifying (27). This shows that we can use only one pilot-symbol at one subcarrier for the whole duration of the channel coherence time to estimate the phase when using the FDS. The overhead of this pilot symbol is negligible compared to the amount of pilots that are required to estimate the channel for coherent detection.

VI. Conclusions

In this paper we have proposed a non-coherent scheme for multiuser massive MIMO-OFDM using differential modulation schemes. We generalized the channel to a doubly dispersive one, and we have provided the analytical expression of SINR for both TDS and FDS. Additionally, we have shown that FDS requires an additional phase estimation and provided a low-overhead method.

The proposed non-coherent massive MIMO-OFDM is useful for the practical implementation of systems which are capable of increasing the capacity and reducing the complexity and latency, as compared to coherent demodulation schemes, since we are avoiding pilot overhead and channel estimation or equalization procedures where prohibitive matrix inversions are involved. The only needed operations for each OFDM symbol are the FFT blocks $\mathcal{O}\left(V(K/2)\log(K)\right)$ and the differential decoding $\mathcal{O}\left(VK\right)$.

Acknowledgment

This work has been funded by project TERESA-ADA (TEC2017-90093-C3-2-R) (MINECO/AEI/FEDER, UE).

References

[1] *Physical channels and modulation (Release 15)*, 3GPP Std. 38.211, 2018.

[2] L. Lu, G. Y. Li, A. L. Swindlehurst, A. Ashikhmin, and R. Zhang, "An overview of Massive MIMO: Benefits and challenges," *IEEE Journal of Selected Topics in Signal Processing*, vol. 8, no. 5, pp. 742–758, Oct 2014.

[3] T. Hwang, C. Yang, G. Wu, S. Li, and G. Y. Li, "OFDM and its wireless applications: A survey," *IEEE Transactions on Vehicular Technology*, vol. 58, no. 4, pp. 1673–1694, May. 2009.

[4] X. Zhu, Z. Wang, C. Qian, L. Dai, J. Chen, S. Chen, and L. Hanzo, "Soft pilot reuse and multicell block diagonalization precoding for massive MIMO systems," *IEEE Transactions on Vehicular Technology*, vol. 65, no. 5, pp. 3285–3298, May 2016.

[5] F. Yang, P. Cai, H. Qian, and X. Luo, "Pilot contamination in massive MIMO induced by timing and frequency errors," *IEEE Transactions on Wireless Communications*, vol. 17, no. 7, pp. 4477–4492, July 2018.

[6] C. Zhang, Y. Jing, Y. Huang, and L. Yang, "Performance analysis for massive MIMO downlink with low complexity approximate zero-forcing precoding," *IEEE Transactions on Communications*, 2018.

[7] J. Flordelis, F. Rusek, F. Tufvesson, E. G. Larsson, and O. Edfors, "Massive mimo performance, TDD versus FDD: What do measurements say?" *IEEE Transactions on Wireless Communications*, vol. 17, no. 4, pp. 2247–2261, April 2018.

[8] A. Manolakos, M. Chowdhury, and A. J. Goldsmith, "CSI is not needed for optimal scaling in multiuser massive SIMO systems," in *2014 IEEE International Symposium on Information Theory*, June 2014, pp. 3117–3121.

[9] A. G. Armada and L. Hanzo, "A non-coherent multi-user large scale SIMO system relaying on M-ary DPSK," in *2015 IEEE International Conference on Communications (ICC)*, June 2015, pp. 2517–2522.

[10] V. M. Baeza, A. G. Armada, M. El-Hajjar, and L. Hanzo, "Performance of a non-coherent massive SIMO M-DPSK system," in *2017 IEEE 86th Vehicular Technology Conference (VTC-Fall)*, Sept 2017, pp. 1–5.

[11] S. Verdu, "Spectral efficiency in the wideband regime," *IEEE Transactions on Information Theory*, vol. 48, no. 6, pp. 1319–1343, Jun 2002.

[12] A. V. Oppenheim and R. W. Schafer, *Discrete-Time Signal Processing*, 3rd ed. Upper Saddle River, NJ, USA: Prentice Hall Press, 2009.